

# Two models for the parametric forcing of a nonlinear oscillator

Nazha Abouhazim · Mohamed Belhaq ·  
Richard H. Rand

Received: 23 January 2006 / Accepted: 14 July 2006 / Published online: 5 January 2007  
© Springer Science + Business Media B.V. 2007

**Abstract** Instabilities associated with 2:1 and 4:1 resonances of two models for the parametric forcing of a strictly nonlinear oscillator are analyzed. The first model involves a nonlinear Mathieu equation and the second one is described by a 2 degree of freedom Hamiltonian system in which the forcing is introduced by the coupling. Using averaging with elliptic functions, the threshold of the overlapping phenomenon between the resonance bands 2:1 and 4:1 (Chirikov's overlap criterion) is determined for both models, offering an approximation for the transition from local to global chaos. The analytical results are compared to numerical simulations obtained by examining the Poincaré section of the two systems.

**Keywords** Parametric excitation · Resonance · Chaos · Elliptic averaging

## 1 Introduction

In this paper, we compare two models for the parametric forcing of a strictly nonlinear oscillator. The unforced

oscillator is of the form

$$\frac{d^2x}{dt^2} + x^3 = 0 \quad (1)$$

The first model, which may be described as a nonlinear Mathieu equation, is of the form

$$\frac{d^2x}{dt^2} + x^3(1 + \varepsilon \cos t) = 0 \quad (2)$$

The second model consists of a 2 degree of freedom Hamiltonian system:

$$\frac{d^2x}{dt^2} + x^3(1 + \varepsilon y) = 0 \quad (3)$$

$$\frac{d^2y}{dt^2} + y = -\varepsilon \frac{x^4}{4} \quad (4)$$

Note that Equation (3) is analogous to Equation (2) if we identify  $y(t)$  with the forcing function  $\cos t$  of (2). However, in the first model (2), the forcing function has constant frequency and constant amplitude, while in the second model (3), (4), the forcing is accomplished by coupling the unforced oscillator (1) to a second oscillator (the “motor”). This takes into account the load on the motor, so that in the second model the forcing function does not have constant frequency or amplitude.

In both models, we will be interested in comparing the instabilities associated with 2:1 and 4:1 resonances.

---

N. Abouhazim · M. Belhaq  
Faculty of Sciences Ain Chock, BP 5366 Maârif,  
Casablanca, Morocco

R. H. Rand (✉)  
Department of Theoretical and Applied Mechanics, Cornell  
University, Ithaca, NY 14853, USA  
e-mail: rhr2@cornell.edu

In particular, this will involve the overlapping phenomenon of the associated resonance bands. To this end, we apply the averaging method to first order in the small parameter  $\varepsilon$  involving Jacobian elliptic functions, and we use Chirikov’s overlap criterion [1], which offers an approximation for the transition from local to global chaos. The critical value of  $\varepsilon$  at which the two resonance bands overlap corresponds to the collision between the separatrices of the two resonance regions emanating from the corresponding hyperbolic fixed points of the Poincaré map.

This collision idea has been implemented to obtain analytical criterion of homoclinic bifurcation in planar and three-dimensional autonomous systems [2, 3]. The objects involved in the collision here are a hyperbolic fixed point and a limit cycle.

In recent paper, Zounes and Rand applied Chirikov’s overlap criterion to investigate the interaction of subharmonic resonances in a quasi-periodic Mathieu equation [4]. They used Lie transform perturbation theory with elliptic functions and derived analytical expressions on parameters at which subharmonic bands in a Poincaré section of action space overlap.

Similar systems to (2), (3), and (4) have been studied, in the case in which the unforced oscillator (1) is linear, and comparisons of the corresponding Poincaré maps have been presented [5].

It is to be noted that the present treatment involves Hamiltonian systems, i.e., systems that have no damping. Although the effect of damping is known to generally reduce resonance response [6], we have not investigated the effect of damping on the Chirikov overlap criterion.

## 2 Nonlinear Mathieu equation

In this section, we use the method of averaging to investigate instabilities in Equation (2) due to 2:1 and 4:1 resonances. The exact solution to (2) involves the Jacobian elliptic function  $\text{cn}$  [7]:

$$x(t) = A \text{cn}(At, k) \tag{5}$$

where  $k = 1/\sqrt{2}$  and  $A$  is the amplitude. The period of  $x(t)$  in  $t$  is  $4K(k)/A$ , where  $K(k)$  is the complete integral of the first kind. As shown in [8, 9], variation of parameters for the equation

$$\frac{d^2x}{dt^2} + x^3 = \varepsilon f \tag{6}$$

takes the form

$$\frac{dA}{dt} = \varepsilon f \frac{\text{cn}'}{A} \tag{7}$$

$$\frac{d\phi}{dt} = \frac{A}{4K} - \varepsilon f \frac{\text{cn}}{4KA^2} \tag{8}$$

Here  $f = -x^3\varepsilon \cos t$ ,  $\text{cn}' = \partial \text{cn}(u, k)/\partial u$  where  $u = 4K\phi$ , and  $\phi = At/4K$ . Hence, the solution of Equation (2) can be written in the form

$$x = A \text{cn}(4K\phi, k) \tag{9}$$

Using the Fourier expansion for  $\text{cn}$  given by Byrd and Friedman [7], we obtain

$$\text{cn}\left(\frac{2K}{\pi}q\right) = 0.955 \cos(q) + 0.043 \cos(3q) + \dots \tag{10}$$

where  $K = K(1/\sqrt{2}) \simeq 1.854$ .

Equation (10) can be replaced by the following approximation

$$\text{cn}\left(\frac{2K}{\pi}q\right) \simeq \cos(q) \tag{11}$$

Using the approximation (11), Equation (9) becomes

$$x = A \cos \theta \quad \text{where} \quad \theta = 2\pi\phi \tag{12}$$

and Equations (7) and (8) become

$$\frac{dA}{dt} = -\varepsilon f \frac{\sin \theta}{A\mu} \tag{13}$$

$$\frac{d\phi}{dt} = \frac{A}{\mu} - \varepsilon f \frac{\cos \theta}{A^2\mu} \tag{14}$$

where  $\mu = 2K/\pi \simeq 1.18$ . Substituting the expression of  $f$  into (13) and (14) via (12), we obtain the following

slow flow

$$\frac{dA}{dt} = \frac{A^2\varepsilon \sin(t + 4\theta)}{16\mu} + \frac{A^2\varepsilon \sin(t + 2\theta)}{8\mu} - \frac{A^2\varepsilon \sin(t - 2\theta)}{8\mu} - \frac{A^2\varepsilon \sin(t - 4\theta)}{16\mu}, \tag{15}$$

$$\begin{aligned} \frac{d\theta}{dt} = & \frac{A\varepsilon \cos(t + 4\theta)}{16\mu} + \frac{A\varepsilon \cos(t + 2\theta)}{4\mu} \\ & + \frac{A\varepsilon \cos(t - 2\theta)}{4\mu} + \frac{A\varepsilon \cos(t - 4\theta)}{16\mu} \\ & + \frac{3A\varepsilon \cos t}{8\mu} + \frac{A}{\mu} \end{aligned} \tag{16}$$

Next, we apply the method of averaging (see [10]). We posit a near-identity transformation for each of the variables  $A, \theta$  as follows

$$A = \bar{A} + \varepsilon W_1(\bar{A}, \bar{\theta}, t) + \mathcal{O}(\varepsilon^2) \tag{17}$$

$$\theta = \bar{\theta} + \varepsilon W_2(\bar{A}, \bar{\theta}, t) + \mathcal{O}(\varepsilon^2) \tag{18}$$

where  $W_1$  and  $W_2$  are the generating functions which will be chosen so as to simplify the resulting slow flow as much as possible. Differentiating (17) and (18), we obtain

$$\begin{aligned} \frac{dA}{dt} &= \frac{d\bar{A}}{dt} + \varepsilon \left( \frac{\partial W_1}{\partial \bar{\theta}} \frac{d\bar{\theta}}{dt} + \frac{\partial W_1}{\partial \bar{A}} \frac{d\bar{A}}{dt} + \frac{\partial W_1}{\partial t} \right) + \mathcal{O}(\varepsilon^2) \end{aligned} \tag{19}$$

$$\begin{aligned} \frac{d\theta}{dt} &= \frac{d\bar{\theta}}{dt} + \varepsilon \left( \frac{\partial W_2}{\partial \bar{\theta}} \frac{d\bar{\theta}}{dt} + \frac{\partial W_2}{\partial \bar{A}} \frac{d\bar{A}}{dt} + \frac{\partial W_2}{\partial t} \right) + \mathcal{O}(\varepsilon^2) \end{aligned} \tag{20}$$

By inspection of Equations (13) and (14), we see that Equations (19) and (20) become, neglecting terms of  $\mathcal{O}(\varepsilon^2)$ ,

$$\frac{dA}{dt} = \frac{d\bar{A}}{dt} + \varepsilon \left( \frac{\partial W_1}{\partial \bar{\theta}} \frac{\bar{A}}{\mu} + \frac{\partial W_1}{\partial t} \right) \tag{21}$$

$$\frac{d\theta}{dt} = \frac{d\bar{\theta}}{dt} + \varepsilon \left( \frac{\partial W_2}{\partial \bar{\theta}} \frac{\bar{A}}{\mu} + \frac{\partial W_2}{\partial t} \right) \tag{22}$$

Now substitute (21) and (22) into Equations (15) and (16) and choose  $W_1$  and  $W_2$  to eliminate as many terms as possible. To eliminate all terms from the right-hand sides of the Equations (15) and (16), we choose  $W_1$  and  $W_2$  as

$$\begin{aligned} W_1(\bar{A}, \bar{\theta}, t) = & -\frac{\bar{A}^2}{16(4\bar{A} + \mu)} \cos(t + 4\theta) \\ & -\frac{\bar{A}^2}{8(2\bar{A} + \mu)} \cos(t + 2\theta) \\ & -\frac{\bar{A}^2}{8(2\bar{A} - \mu)} \cos(t - 2\theta) \\ & -\frac{\bar{A}^2}{16(4\bar{A} - \mu)} \cos(t - 4\theta) \end{aligned} \tag{23}$$

and

$$\begin{aligned} W_2(\bar{A}, \bar{\theta}, t) = & -\frac{(4 - \mu)\bar{A}^2 + \mu\bar{A}}{16(4\bar{A} + \mu)^2} \cos(t + 4\theta) \\ & -\frac{(4 - \mu)\bar{A}^2 + 2\mu\bar{A}}{8(2\bar{A} + \mu)^2} \cos(t + 2\theta) \\ & -\frac{(4 - \mu)\bar{A}^2 + 2\mu\bar{A}}{8(2\bar{A} - \mu)^2} \cos(t - 2\theta) \\ & -\frac{(4 - \mu)\bar{A}^2 + \mu\bar{A}}{16(4\bar{A} - \mu)^2} \cos(t - 4\theta) \end{aligned} \tag{24}$$

The resulting (non-resonant) slow flow is given by

$$\frac{d\bar{A}}{dt} = 0 \tag{25}$$

$$\frac{d\bar{\theta}}{dt} = \frac{\bar{A}}{\mu} \tag{26}$$

Note that Equations (23) and (24) have vanishing denominators when  $A = \mu/2$  or  $A = \mu/4$ , which means that the terms with  $\sin / \cos(t - 2\theta)$  and  $\sin / \cos(t - 4\theta)$  are resonant. We investigate these cases next.

### 2.1 The 2:1 resonance

In order to investigate what happens close to the 2:1 resonance, that is, when  $A \approx \mu/2 = 0.59$ , we omit removing the terms which cause the resonance. Writing

$\psi = 2\theta - t$ , Equations (23) and (24) become

$$\frac{dA}{dt} = \frac{\varepsilon A^2 \sin(\psi)}{8\mu}, \tag{27}$$

$$\frac{d\psi}{dt} = -\frac{-\varepsilon A \cos(\psi) + 2\mu - 4A}{2\mu} \tag{28}$$

Equilibria of the slow flow (27) and (28) correspond to periodic motions in the original Equation (2). The condition for equilibrium is  $(dA)/(dt) = (d\psi)/(dt) = 0$ , which gives from Equation (27)

$$\psi = 0 \quad \text{or} \quad \psi = \pi \tag{29}$$

Substituting (29) into the right-hand side of (28) and solving for  $A$ , we obtain

$$\left( \psi_0 = 0, \quad A_{21-} = \frac{2\mu}{\varepsilon + 4} \right) \quad \text{and} \tag{30}$$

$$\left( \psi_\pi = \pi, \quad A_{21+} = \frac{2\mu}{4 - \varepsilon} \right)$$

Next we investigate the stability of these slow flow equilibria. The Jacobian matrix of the slow flow (27) and (28) gives  $\text{tr}(J) = 0$  and  $\text{det}(J) < 0$  for  $(A_{21-}, 0)$  which is therefore a saddle and  $\text{tr}(J) = 0$  and  $\text{det}(J) > 0$  for  $(A_{21+}, \pi)$  which is a center.

In order to determine the equation of the separatrix, we divide Equation (27) by Equation (28)

$$\frac{dA}{d\psi} = -\frac{\varepsilon A^2 \sin(\psi)}{4(-\varepsilon A \cos(\psi) + 2\mu - 4A)} \tag{31}$$

and integrate Equation (31). Using the condition that the separatrix passes through the saddle point to evaluate the constant of integration, we obtain the following equation

$$\frac{A^4(3\varepsilon \cos(\psi) + 12) - 8A^3\mu}{3} \mu = -\frac{16\mu^4}{3(\varepsilon + 4)^3} \tag{32}$$

To determine the thickness of the 2:1 resonance band, we consider a point  $A^*$  which is located at  $\psi = \pi$ , being a vertical distance  $r_{21}$  from the center:

$$A^* = A_{21+} + r_{21} \tag{33}$$

where  $A_{21+}$  is given by (30). Introducing (33) into (32) and solving for  $r_{21}$ , we obtain

$$2r_{21} = \frac{\mu\sqrt{\varepsilon}}{2} \tag{34}$$

where  $\mu = 1.18$ . This gives the value of the thickness  $2r_{21}$  of the 2 : 1 resonance band as a function of  $\varepsilon$ .

### 2.2 The 4:1 resonance

Following the same analysis as was done for the 2:1 resonance, we now omit removing terms which cause the 4:1 resonance in the slow flow (15) and (16), which gives

$$\frac{dA}{dt} = \frac{\varepsilon A^2 \sin(\psi)}{16\mu}, \tag{35}$$

$$\frac{d\psi}{dt} = -\frac{-\varepsilon A \cos(\psi) + 4\mu - 16A}{4\mu} \tag{36}$$

Equilibria of the slow flow (35) and (36) again correspond to periodic motions in the original Equation (2), and are now given by

$$\left( \psi_0 = 0, \quad A_{41-} = \frac{4\mu}{\varepsilon + 16} \right) \quad \text{and} \tag{37}$$

$$\left( \psi_\pi = \pi, \quad A_{41+} = \frac{4\mu}{16 - \varepsilon} \right)$$

where  $(A_{41-}, 0)$  is a saddle and  $(A_{41+}, \pi)$  is a center.

In order to determine the equation of the separatrix, we divide Equation (35) by Equation (36)

$$\frac{dA}{d\psi} = -\frac{\varepsilon A^2 \sin(\psi)}{4(-\varepsilon A \cos(\psi) + 4\mu - 16A)} \tag{38}$$

and we integrate Equation (38). Again using the condition that the separatrix passes through the saddle point, we obtain

$$\frac{A^4(3\varepsilon \cos(\psi) + 48) - 16A^3\mu}{3} = -\frac{256\mu^4}{3(\varepsilon + 16)^3} \tag{39}$$

The thickness of the 4:1 resonance band is obtained by considering a point  $A^*$  which is located at  $\psi = \pi$ , being a vertical distance  $r_{41}$  from the center:

$$A^* = A_{41+} + r_{41} \tag{40}$$

where  $A_{41+}$  is given by (37). Introducing (40) into (39) and solving for  $r_{41}$ , we obtain

$$2r_{41} = \frac{\mu\sqrt{\varepsilon}}{8} \tag{41}$$

where  $\mu = 1.18$ . This gives the value of the thickness  $2r_{41}$  of the 4:1 resonance band as a function of  $\varepsilon$ .

### 2.3 Overlap criterion

In this section, we apply Chirikov’s overlap criterion [1] to derive a value for  $\varepsilon$  at which the two primary subharmonic resonance bands (2:1 and 4:1) first overlap. As  $\varepsilon$  is increased, the two zones will first overlap when the minimum  $A$  for the 2:1 resonance band reaches the maximum  $A$  for the 4:1 resonance band

$$A_{21+} - r_{21} = A_{41+} + r_{41} \tag{42}$$

From (30), (34), (37), and (41), we obtain the following equation on  $\varepsilon$

$$\frac{2\mu}{4 - \varepsilon} - \frac{\mu\sqrt{\varepsilon}}{4} = \frac{4\mu}{16 - \varepsilon} + \frac{\mu\sqrt{\varepsilon}}{16} \tag{43}$$

By neglecting terms of  $\mathcal{O}(\varepsilon)$  and solving (43) for  $\varepsilon$ , we obtain an approximation for  $\varepsilon_c$ , which is the critical value of  $\varepsilon$  corresponding to a transition from local to global chaos:

$$\varepsilon_c = 0.64 \tag{44}$$

In Fig. 1, we show the 2 : 1 and 4 : 1 resonance bands in the  $(\theta, A)$  phase space given by Equations (32) and (39). Figure 2 displays the growth of these resonance bands as  $\varepsilon$  increases.

Figure 3 illustrates the Poincaré section of Equation (2) for  $\varepsilon = 0.1$ , displayed in the  $(x, \dot{x})$  plane and obtained by numerical integration of Equation (2). Figures 4 and 5 show comparable Poincaré sections for  $\varepsilon = 0.3, 0.4, 0.5$ , and  $0.6$ . From these figures, we can see the growth of 2:1 and 4:1 resonance bands as  $\varepsilon$  increases. In Fig. 4, we see local chaos appearing near the saddles. Figure 5 shows the mechanism of overlapping between the 2:1 and 4:1 resonance bands.

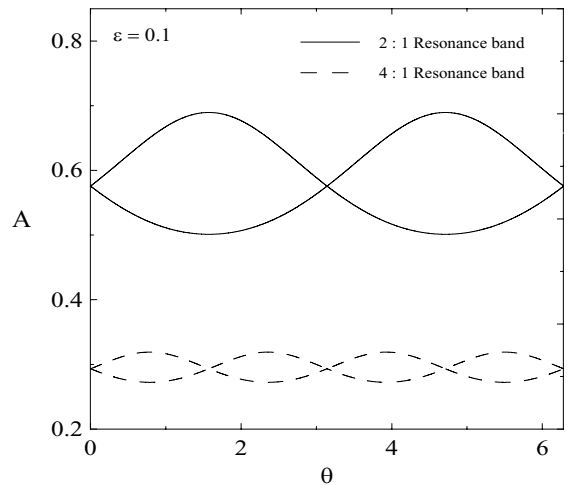


**Fig. 1** The 2:1 and 4:1 resonance bands in the  $(\theta, A)$  plane given by Equation (32), with  $\psi = 2\theta$ , and Equation (39), with  $\psi = 4\theta$ , for  $\varepsilon = 0.1$

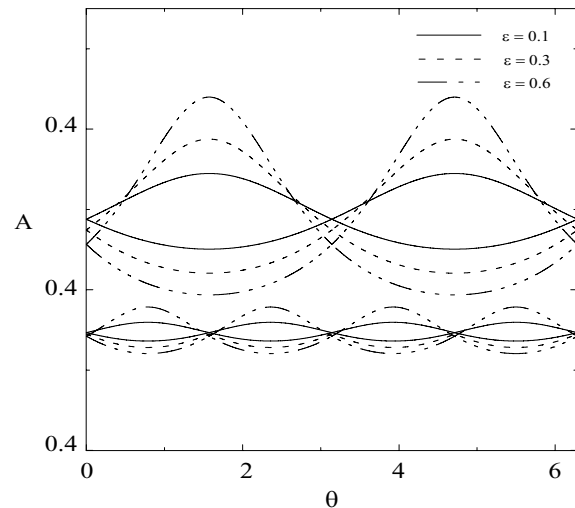
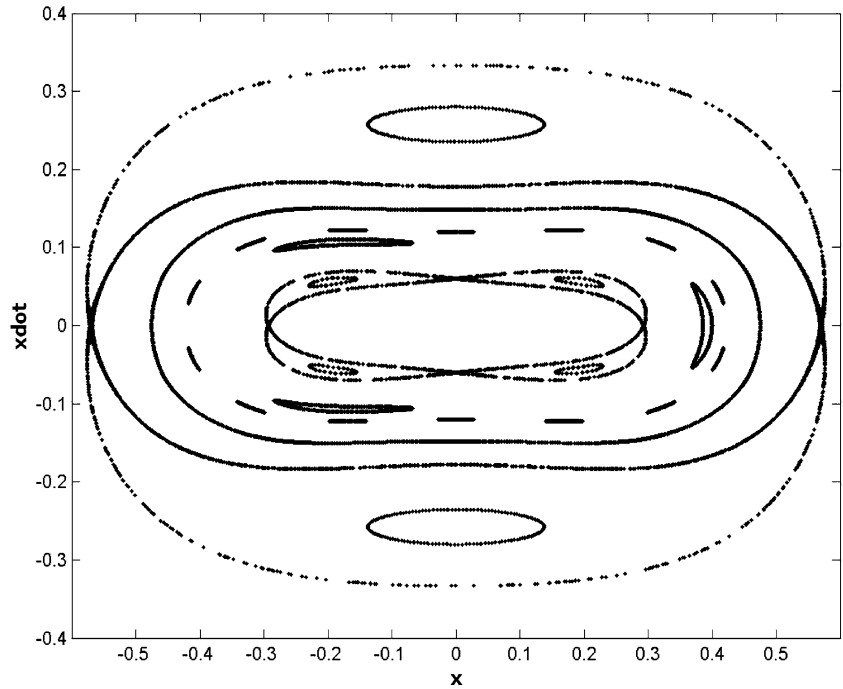


**Fig. 2** The 2:1 and 4:1 resonance bands in the  $(\theta, A)$  plane given by Equation (32), with  $\psi = 2\theta$ , and Equation (39), with  $\psi = 4\theta$ , for various values of  $\varepsilon$

### 3 Two coupled nonlinear oscillators

In this section, we use averaging to investigate instabilities in Equations (3) and (4) due to 2:1 and 4:1 resonances. Note that Equations (3) and (4) are a Hamiltonian system. For such systems KAM theory [11] tells us that local chaos exists in the neighborhood of resonances. As  $\varepsilon$  is increased, the KAM picture of local pockets of chaos separated by invariant tori becomes inapplicable and is replaced by global chaos.

**Fig. 3** Poincaré section in the  $(x, \dot{x})$  plane obtained by numerically integrating Equation (2) with  $\varepsilon = 0.1$ . Note the presence of the large 2:1 resonance band (characterized by two saddles and two centers) and the small 4:1 resonance band (characterized by four saddles and four centers). In between these two can be seen part of a 3:1 resonance band (not treated in this paper)



The Hamiltonian of the system (3) and (4) has the form

$$H = \frac{\dot{x}^2}{2} + \frac{\dot{y}^2}{2} + \frac{x^4}{4} + \frac{y^2}{2} + \varepsilon \frac{x^4}{4} y \tag{45}$$

For the unperturbed system ( $\varepsilon = 0$ ), Equations (3) and (4) become

$$\frac{d^2x}{dt^2} + x^3 = 0 \tag{46}$$

$$\frac{d^2y}{dt^2} + y = 0 \tag{47}$$

and the Hamiltonian becomes

$$H = \frac{\dot{x}^2}{2} + \frac{\dot{y}^2}{2} + \frac{x^4}{4} + \frac{y^2}{2} \tag{48}$$

The exact solutions to Equations (46) and (47) are given by

$$x = A \operatorname{cn}(At, k), \quad k = 1/\sqrt{2} \tag{49}$$

$$y = R \cos \psi \tag{50}$$

Substituting Equations (49) and (50) into Equation (48), we obtain

$$H = \frac{R^2}{2} + \frac{A^4}{4} \tag{51}$$

As shown earlier, Equation (49) may be approximated by

$$x = A \cos \theta \tag{52}$$

Here  $\theta = 2\pi\phi$  and  $\phi = At/4K$ ,  $\mu = 2K/\pi$  where  $K = K(k) \simeq 1.854$  is the elliptic integral of the first kind.

As shown in [9], variation of parameters for the equations

$$\frac{d^2x}{dt^2} + x^3 = \varepsilon f \tag{53}$$

$$\frac{d^2y}{dt^2} + y = \varepsilon g \tag{54}$$

takes the form

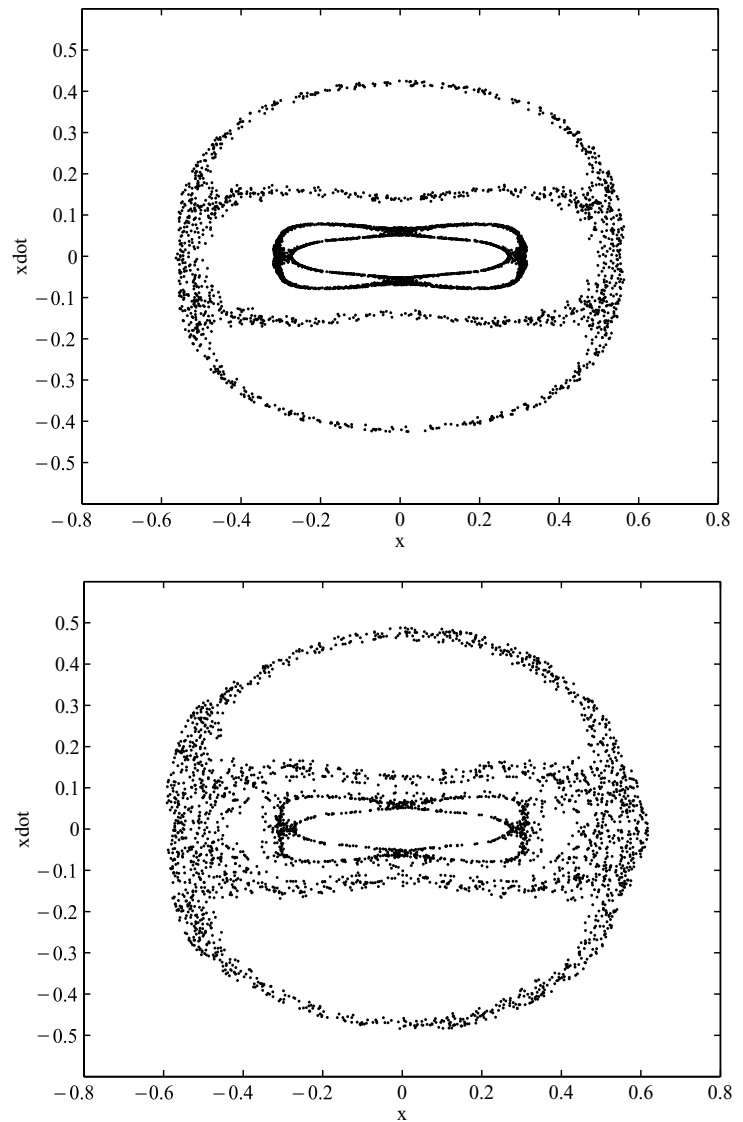
$$\frac{dA}{dt} = -\varepsilon f \frac{\sin \theta}{A\mu} \tag{55}$$

$$\frac{d\theta}{dt} = \frac{A}{\mu} - \varepsilon f \frac{\cos \theta}{A^2\mu} \tag{56}$$

$$\frac{dR}{dt} = -\varepsilon g \sin \psi \tag{57}$$

$$\frac{d\psi}{dt} = 1 - \varepsilon g \frac{\cos \psi}{R} \tag{58}$$

**Fig. 4** Poincaré section in the  $(x, \dot{x})$  plane obtained by numerically integrating Equation (2) with  $\varepsilon = 0.3$  (top) and  $\varepsilon = 0.4$  (bottom). Note the growth of the 2 : 1 and 4 : 1 resonance bands and the appearance of local chaos near the saddles



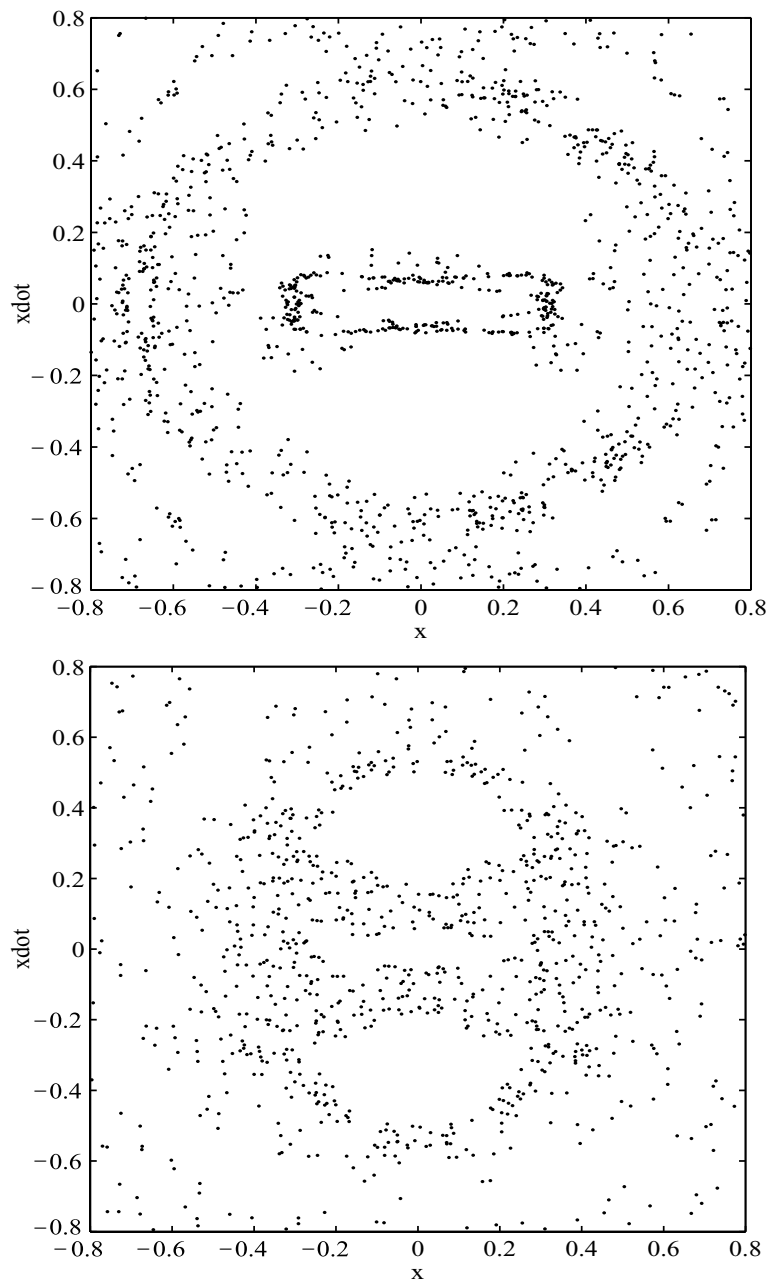
Now we take  $f = -x^3y$  and  $g = -x^4/4$  and substitute for  $x$  and  $y$  their expressions given in (49) and (50), then expand and reduce the trig terms, whereupon Equations (55) through (58) become

$$\begin{aligned} \frac{dA}{dt} = & \frac{\varepsilon R A^2 \sin(\psi + 4\theta)}{16\mu} \\ & + \frac{\varepsilon R A^2 \sin(\psi + 2\theta)}{8\mu} - \frac{\varepsilon R A^2 \sin(\psi - 2\theta)}{8\mu} \\ & - \frac{\varepsilon R A^2 \sin(\psi - 4\theta)}{16\mu} \end{aligned} \tag{59}$$

$$\begin{aligned} \frac{d\theta}{dt} = & \frac{\varepsilon R A \cos(\psi + 4\theta)}{16\mu} + \frac{\varepsilon R A \cos(\psi + 2\theta)}{4\mu} \\ & + \frac{\varepsilon R A \cos(\psi - 2\theta)}{4\mu} + \frac{\varepsilon R A \cos(\psi - 4\theta)}{16\mu} \\ & + \frac{3\varepsilon A R \cos(\psi)}{8\mu} + \frac{A}{\mu} \end{aligned} \tag{60}$$

$$\begin{aligned} \frac{dR}{dt} = & \frac{\varepsilon A^4 \sin(\psi + 4\theta)}{64\mu} + \frac{\varepsilon A^4 \sin(\psi + 2\theta)}{16\mu} \\ & + \frac{\varepsilon A^4 \sin(\psi - 2\theta)}{16\mu} + \frac{\varepsilon A^4 \sin(\psi - 4\theta)}{64\mu} \\ & + \frac{3\varepsilon A^4 \sin(\psi)}{32} \end{aligned} \tag{61}$$

**Fig. 5** Poincaré section in the  $(x, \dot{x})$  plane obtained by numerically integrating Equation (2) with  $\varepsilon = 0.5$  (top) and  $\varepsilon = 0.6$  (bottom). Note that the 2 : 1 and 4 : 1 resonance bands begin to touch at  $\varepsilon = 0.5$  and become globally chaotic at  $\varepsilon = 0.6$



$$\begin{aligned}
 \frac{d\psi}{dt} = & \frac{\varepsilon A^4 \cos(\psi + 4\theta)}{64R} + \frac{\varepsilon A^4 \cos(\psi + 2\theta)}{16R} \\
 & + \frac{\varepsilon A^4 \cos(\psi - 2\theta)}{16R} + \frac{\varepsilon A^4 \cos(\psi - 4\theta)}{64R} \\
 & + \frac{3\varepsilon A^4 \cos(\psi)}{32R} + 1
 \end{aligned} \tag{62}$$

### 3.1 The 2:1 resonance

As in the case of the first model presented earlier, we apply the method of averaging to these equations. Specifically, we posit a near identity transformation for each of the variables  $R$ ,  $A$ ,  $\psi$ , and  $\theta$ , and we choose the generating functions to remove all the terms except those

which represent a resonance. We begin with the 2 : 1 resonance and write the Equations (59) and (62) in the form

$$\frac{dA}{dt} = -\frac{\varepsilon R A^2 \sin v}{8\mu} \tag{63}$$

$$\frac{dR}{dt} = \frac{\varepsilon A^4 \sin v}{16} \tag{64}$$

$$\frac{dv}{dt} = -\frac{\varepsilon A R \cos v}{2\mu} + \frac{\varepsilon A^4 \cos v}{16R} - \frac{2A}{\mu} + 1 \tag{65}$$

where  $v = 2\theta - \psi$ .

This three-dimensional system can be simplified by dividing Equation (64) by Equation (63), giving

$$\frac{dR}{dA} = -\frac{\mu A^2}{2R} \tag{66}$$

Integrating Equation (66), we obtain the first integral

$$\frac{R^2}{2} + \frac{\mu A^3}{6} = k_1 = \text{constant} \tag{67}$$

A second first integral is

$$8R^2 + 4A^4 + \varepsilon A^4 R \cos v = k_2 = \text{constant} \tag{68}$$

Equilibria of the slow flow Equations (63)–(65) correspond to periodic motions in the original Equations (3) and (4). In order to obtain expressions for the slow flow equilibria and to investigate their stability, we proceed as follows: we solve Equation (67) for  $R$  and substitute the resulting expression in Equations (63) and (65) to obtain two equations in  $A$  and  $v$  of the form

$$\frac{dA}{dt} = -\frac{\varepsilon \sqrt{2k_1 - \mu A^3/3} A^2 \sin v}{8\mu} \tag{69}$$

$$\begin{aligned} \frac{dv}{dt} = & -\frac{\varepsilon A \sqrt{2k_1 - \mu A^3/3} \cos v}{2\mu} \\ & + \frac{\varepsilon A^4 \cos v}{16\sqrt{2k_1 - \mu A^3/3}} - \frac{2A}{\mu} + 1 \end{aligned} \tag{70}$$

Equilibria in Equations (69) and (70) may be obtained by setting the right-hand sides equal to zero, giving

$$v = 0 \quad \text{or} \quad v = \pi \tag{71}$$

In the case of the 2:1 resonance, we set

$$A = \frac{\mu}{2} + \varepsilon u \tag{72}$$

We substitute (72) into the right-hand side of (70), and we solve for  $u$ , giving

for  $v = 0$ ,

$$u = -\frac{\sqrt{48k_1 - \mu^4}(11\sqrt{6}\mu^5 - 384\sqrt{6}k_1\mu)}{768\mu^4 - 36864k_1}, \tag{73}$$

for  $v = \pi$ ,

$$u = \frac{\sqrt{48k_1 - \mu^4}(11\sqrt{6}\mu^5 - 384\sqrt{6}k_1\mu)}{768\mu^4 - 36864k_1}. \tag{74}$$

Linearizing in the neighborhood of these equilibria, we find that  $v = 0$  is a saddle while  $v = \pi$  is a center. To determine the equation of the separatrix, we eliminate  $R$  from Equation (68) using Equation (67) to find

$$\begin{aligned} A^4 \varepsilon \sqrt{2k_1 - A^3 \mu/3} \cos v + 8(2k_1 - A^3 \mu/3) \\ + 4A^4 = k_2 \end{aligned} \tag{75}$$

We choose  $k_2$  so that the separatrix passes through the saddle at  $v = 0$ . This gives the following value for  $k_2$

$$k_2 = \frac{(192k_1 - \mu^4)}{12} + \varepsilon \frac{\sqrt{6}\sqrt{48k_1 - \mu^4} \mu^4}{192} + O(\varepsilon^2) \tag{76}$$

In order to determine the width of the separatrix at  $v = \pi$ , we substitute Equation (76) into Equation (75), then set  $v = \pi$  and  $A = \mu/2 + \sqrt{\varepsilon} D_{21}/2$ , where  $D_{21}$  represents the width of the separatrix to  $O(\sqrt{\varepsilon})$ . We obtain

$$D_{21} = \left( \frac{\mu^2 \sqrt{48k_1 - \mu^4}}{8\sqrt{6}} \right)^{1/2} \tag{77}$$

### 3.2 The 4:1 resonance

Following the same analysis as for the 2 : 1 resonance, the slow flow that describes the dynamics close to the

4 : 1 resonance is given by

$$\frac{dA}{dt} = -\frac{\varepsilon R A^2 \sin v}{16\mu} \tag{78}$$

$$\frac{dR}{dt} = \frac{\varepsilon A^4 \sin v}{64} \tag{79}$$

$$\frac{dv}{dt} = -\frac{\varepsilon A R \cos v}{4\mu} + \frac{\varepsilon A^4 \cos v}{64R} - \frac{4A}{\mu} + 1 \tag{80}$$

where  $v = 4\theta - \psi$ .

We simplify this three-dimensional system by dividing Equation (79) by Equation (78) to obtain

$$\frac{dR}{dA} = -\frac{\mu A^2}{2R} \tag{81}$$

Integrating Equation (81) yields

$$\frac{R^2}{2} + \frac{\mu A^3}{12} = k_3 = \text{constant} \tag{82}$$

A second first integral is

$$32R^2 + 16A^4 + \varepsilon A^4 R \cos v = k_4 = \text{constant} \tag{83}$$

Equilibria of the slow flow equations (78)–(80) correspond to periodic motions in the original Equations (3) and (4). In order to obtain expressions for the slow flow equilibria and to investigate their stability, we proceed as follows: we solve Equation (82) for  $R$  and substitute the resulting expression in Equations (78) and (80) to obtain two equations on  $A$  and  $v$ .

The equilibria are similar to the 2:1 case:  $v = 0$  is a saddle and  $v = \pi$  is a center. Moreover, the variable  $u$  is now defined by

$$A = \frac{\mu}{4} + \varepsilon u \tag{84}$$

To determine the equation of the separatrix, we eliminate  $R$  from Equation (83) using Equation (82). This leads to

$$A^4 \varepsilon \sqrt{2k_3 - A^3 \mu / 6} \cos v + 32(2k_3 - A^3 \mu / 6) + 16A^4 = k_4 \tag{85}$$

We choose  $k_4$  so that the separatrix passes through the saddle at  $v = 0$ , giving

$$k_4 = \frac{(3072k_3 - \mu^4)}{48} + \varepsilon \frac{\sqrt{6} \sqrt{768k_3 - \mu^4} \mu^4}{12288} + O(\varepsilon^2) \tag{86}$$

In order to determine the width of the separatrix at  $v = \pi$ , we substitute Equation (86) into Equation (85), then set  $v = \pi$  and  $A = \mu/4 + \sqrt{\varepsilon} D_{41}/2$ , where  $D_{41}$  is the width of the separatrix to  $O(\sqrt{\varepsilon})$ . We obtain

$$D_{41} = \left( \frac{\mu^2 \sqrt{768k_3 - \mu^4}}{512\sqrt{6}} \right)^{1/2} \tag{87}$$

### 3.3 Overlap criterion

Now we apply Chirikov’s overlap criterion to derive an approximate value for  $\varepsilon$  at which the two primary subharmonic resonance bands (2:1 and 4:1) first overlap. Equating the minimum  $A$  for the 2:1 resonance band to the maximum  $A$  for the 4 : 1 resonance band leads to

$$\frac{\mu}{2} - \sqrt{\varepsilon} \frac{D_{21}}{2} = \frac{\mu}{4} + \sqrt{\varepsilon} \frac{D_{41}}{2} \tag{88}$$

Substituting Equations (77) and (87) into Equation (88) and solving in  $\varepsilon$ , we find the following expression for  $\varepsilon_c$

$$\varepsilon_c = \frac{128\sqrt{6}}{[(768k_3 - \mu^4)^{1/4} + 8(48k_1 - \mu^4)^{1/4}]^2} \tag{89}$$

Note that the critical value of  $\varepsilon$  depends on the value of the constants  $k_1$  and  $k_3$  which will correspond to the energy  $h$  given by the Equation (51). Thus, from Equations (51), (67), and (82) we have

$$k_1 = h - \frac{A^4}{4} + \frac{\mu A^3}{6} \tag{90}$$

$$k_3 = h - \frac{A^4}{4} + \frac{\mu A^3}{12} \tag{91}$$

Next we set  $A = \mu/2$  in Equation (90), which is valid close to the 2:1 resonance, and  $A = \mu/4$  in Equation (91) which is valid close to the 4:1 resonance. Equations (90) and (91) become

$$k_1 = h + \frac{\mu^4}{192} \tag{92}$$

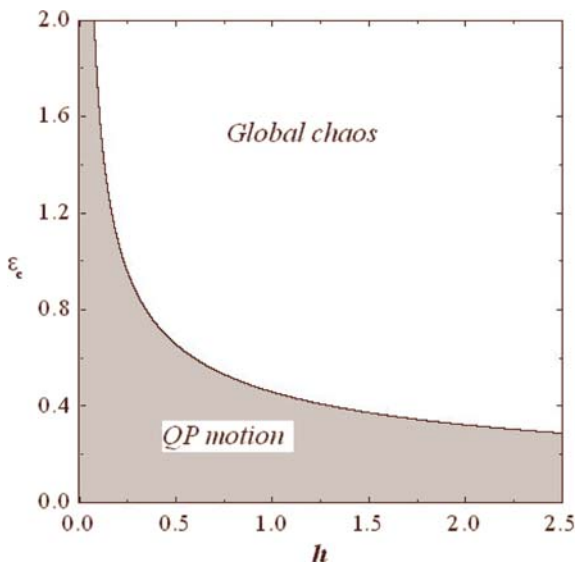
$$k_3 = h + \frac{\mu^4}{3072} \tag{93}$$

Substituting Equations (92) and (93) into Equations (89), we obtain

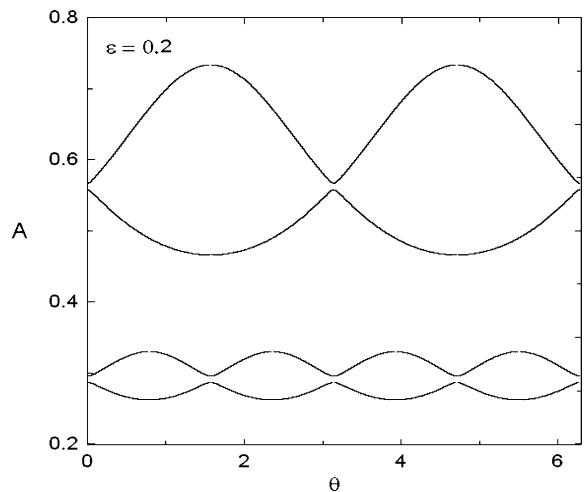
$$\varepsilon_c = \frac{256\sqrt{2}}{[\sqrt{1024h - \mu^4} + 16(64h - \mu^4)^{1/4} (1024h - \mu^4)^{1/4} + 64\sqrt{64h - \mu^4}]} \tag{94}$$

Figure 6 displays the critical parameter value  $\varepsilon_c$  versus  $h$  given by Equation (94). It shows that for small values of  $\varepsilon$ , the system needs high energy to achieve global chaos.

In Figure 7, we show the 2 : 1 and 4 : 1 resonance bands in the  $(\theta, A)$  phase space given by Equations (75) and (85). Figure 8 displays the growth of these resonance bands as  $\varepsilon$  increases.



**Fig. 6**  $\varepsilon_c$  versus  $h$  giving the transition curve (94) from quasi-periodic motion and local chaos to global chaos



**Fig. 7** The 2 : 1 and 4 : 1 resonance bands in the  $(\theta, A)$  plane given by Equation (75), with  $v = 2\theta$ , and Equation (85), with  $v = 4\theta$ , for  $\varepsilon = 0.2$

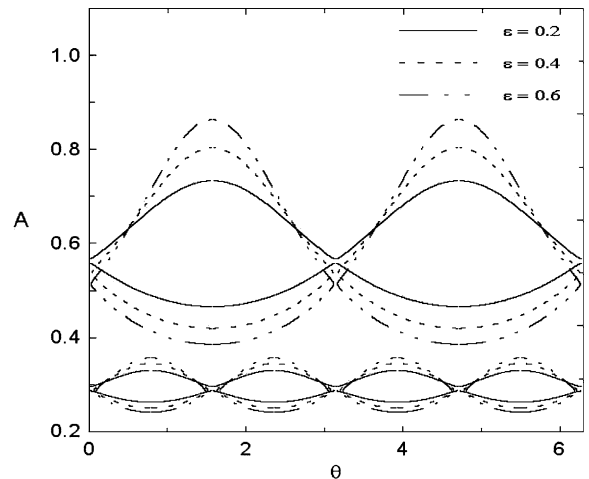
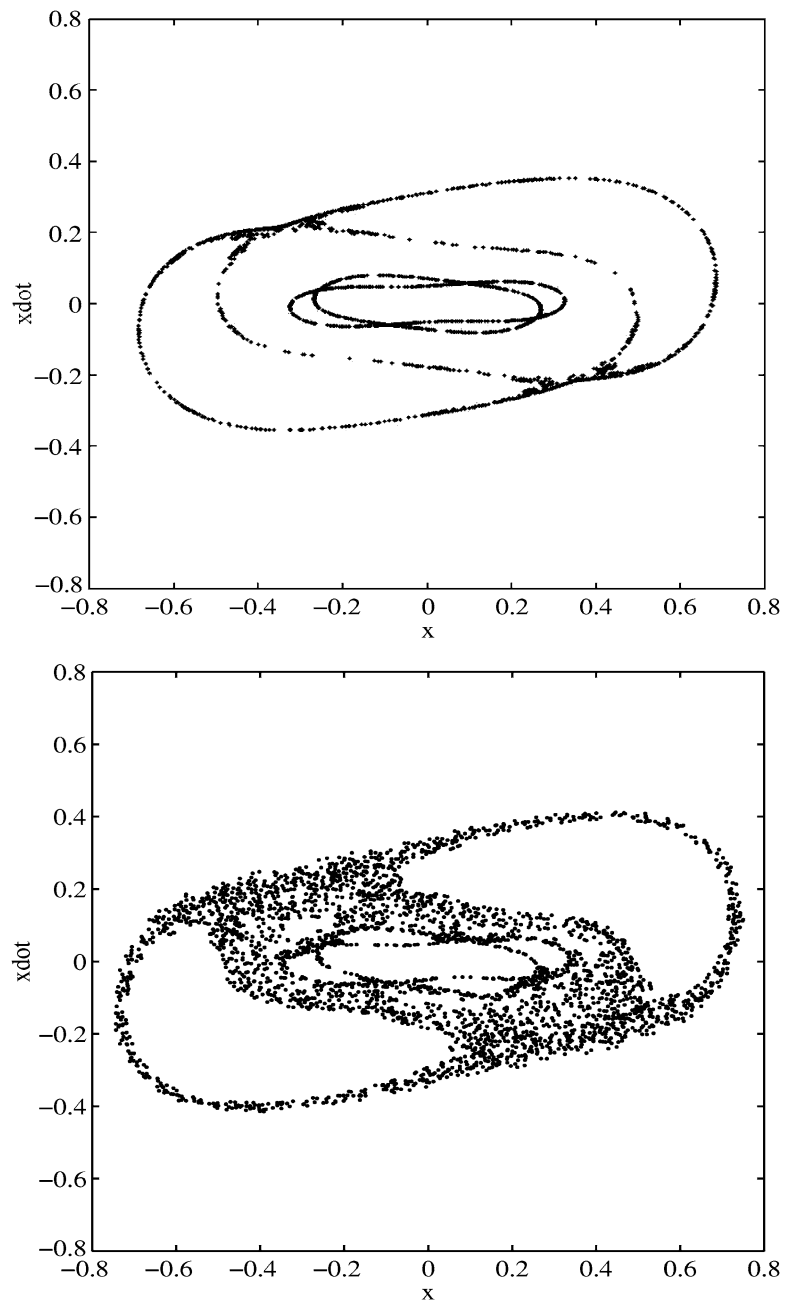


**Fig. 8** The 2 : 1 and 4 : 1 resonance bands in the  $(\theta, A)$  plane given by Equation (75), with  $v = 2\theta$ , and Equation (85), with  $v = 4\theta$ , for different values of  $\varepsilon$

Figures 9–10 show the results of numerical integration of Equations (3) and (4). These figures show the mechanism of overlapping between the 2:1 and 4:1 resonance bands in the Poincaré section when  $\varepsilon$  is varied for fixed  $h = 0.53$ , for which Equation (94) gives  $\varepsilon_c = 0.636$ . This value of  $h$  was arrived at by comparing Hamiltonians in the two models, and identifying  $y$  with  $\cos t$ . The Hamiltonian for the first model, Equation (2), is given by:

$$H_1 = \frac{\dot{x}^2}{2} + \frac{x^4}{4} + \varepsilon \frac{x^4}{4} \cos t \tag{95}$$

**Fig. 9** The Poincaré section of the system (3) and (4), in the  $(x, \dot{x})$  plane, displays the growth of resonance bands 2 : 1 and 4 : 1 when  $\varepsilon$  increases. Here  $\varepsilon = 0.2$  (*top*) and  $\varepsilon = 0.4$  (*bottom*)

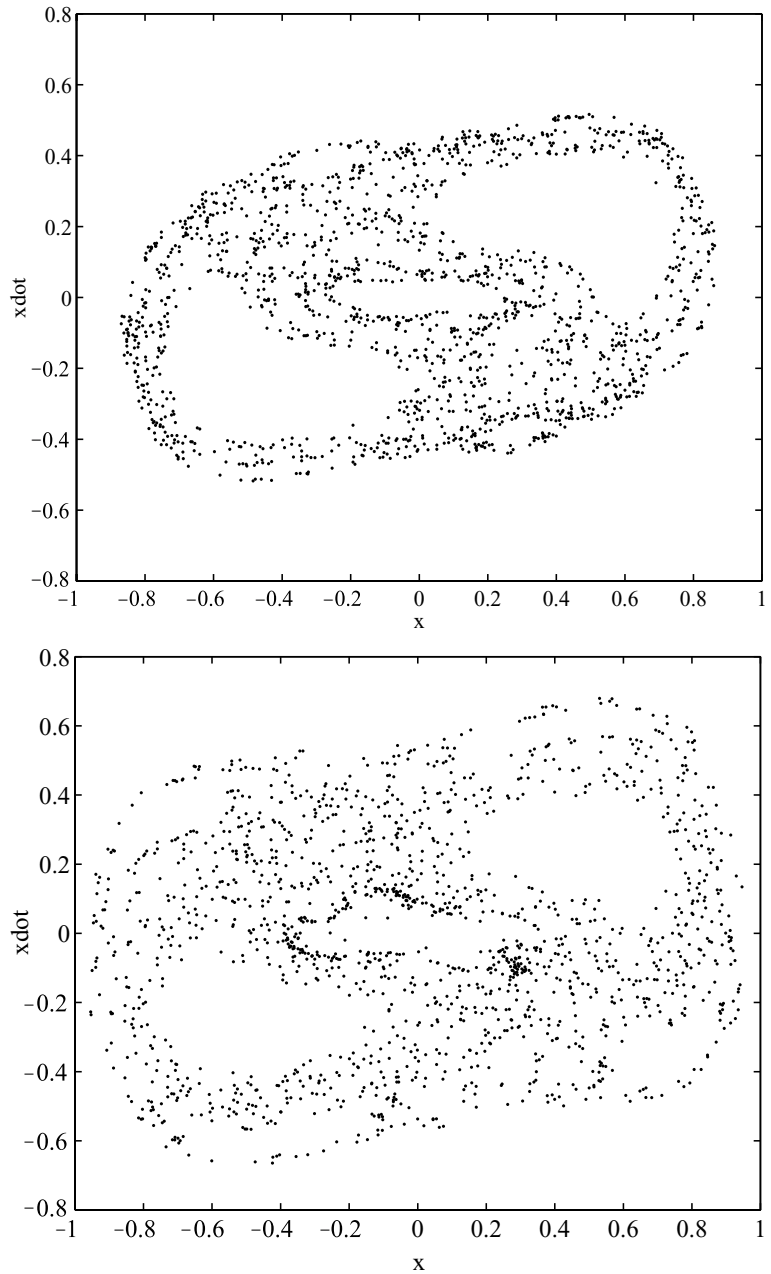


The Hamiltonian for the second model, Equation (45), is given by

$$H_2 = \frac{\dot{x}^2}{2} + \frac{\dot{y}^2}{2} + \frac{x^4}{4} + \frac{y^2}{2} + \varepsilon \frac{x^4}{4} y \quad (96)$$

If we replace  $y$  in (96) by  $\cos t$ , we see that  $H_2 = H_1 + 0.5$ . Now if we take  $H_1$  to correspond to the amplitude  $A$  of 2:1 resonance, i.e., to  $A_{2:1 \text{ resonance}} \simeq \mu/2$ , then we find that  $H_1 \simeq A_{2:1 \text{ resonance}}^4/4 = 0.030$  and hence that  $H_2 = 0.53$ .

**Fig. 10** Overlap phenomenon between the two resonance bands 2 : 1 and 4 : 1 in the Poincaré section when  $\varepsilon$  is varied for fixed value of  $h$ . Here  $\varepsilon = 0.5$  (*top*) and  $\varepsilon = 0.6$  (*bottom*)



#### 4 Conclusions

In this work, we investigate the overlapping phenomenon associated with 2:1 and 4:1 resonances for two parametric forcing models. The first model is described by a nonlinear Mathieu equation. The second one consists of a 2 degree of freedom Hamiltonian

system analogous to the first model in the sense that the forcing is due to the coupling. In both models, we have focused our attention on the comparison of the critical value of  $\varepsilon$  at which the two resonance bands 2:1 and 4:1 overlap resulting the transition from local to global chaos in the systems.

In the first system,  $\varepsilon$  corresponds to the amplitude of the parametric excitation, while in the second system,  $\varepsilon$  refers to the coupling coefficient. Increasing this parameter, in both models, increases the size of the resonance bands in the Poincaré section.

Note that  $\varepsilon_c$ , the critical value of  $\varepsilon$ , in the second model depends on energy  $h$ , whereas  $\varepsilon_c$  does not depend on the energy in the first model. This is because the amplitude of the forcing function in the second model is not constant (as it is in the first model), but rather it depends upon the amplitude of the response variable,  $A$ , representing the load on the motor variable. This is related to the fact that the resonance instabilities in the first model are due to parametric excitation, whereas in the second model they are due to *autoparametric excitation* [12], that is, parametric excitation which is caused by the system itself, rather than by an external periodic driver.

If the analytically derived values for Chirikov's approximation for the transition from local to global chaos are compared with the results obtained by numerical integration of the original equations of motion, we find that the analytic result is high. For example, in the case of the first model, Equation (44) gave

$$\varepsilon_c = 0.64 \quad (97)$$

whereas Fig. 5 shows that global chaos has already occurred at  $\varepsilon = 0.6$ . This effect may be explained by noting that there are many smaller resonances which can help to make a chaos bridge between the 2:1 and the 4:1 resonance regions. If our analysis were to take such intermediate resonances into account, the resulting value of  $\varepsilon_c$  would be lower.

**Acknowledgements** This work was supported by NSF International Travel Grant INT-9906084. The hospitality of the Department of Theoretical and Applied Mechanics of Cornell University is gratefully acknowledged.

## References

1. Chirikov, B.V.: A universal instability of many-dimensional oscillator systems. *Phys. Rep.* **52**, 263–379 (1979)
2. Belhaq, M., Lakrad, F.: Prediction of homoclinic bifurcation: the elliptic averaging method. *Chaos Solitons Fractals* **11**, 2251–2258 (2000)
3. Belhaq, M., Lakrad, F.: Analytics of homoclinic bifurcations in three-dimensional systems. *Int. J. Bif. Chaos* **12**, 2479–2486 (2002)
4. Zounes, R.S., Rand, R.H.: Global behavior of a nonlinear quasiperiodic Mathieu equation. *Nonlinear Dyn.* **27**, 87–105 (2002)
5. Holmes, C.A., Rand, R.H.: Coupled oscillators as a model for nonlinear parametric excitation. *Mech. Res. Comm.* **8**(5), 263–268 (1981)
6. Rand, R.H.: *Lecture Notes on Nonlinear Vibrations*, version 52 (2005). Available on-line at <http://www.tam.cornell.edu/randdocs/nlvibe52.pdf>
7. Byrd, P., Friedman, M.: *Handbook of Elliptic Integrals for Engineers and Scientists*. Springer, Berlin (1954)
8. Coppola, V.T., Rand, R.H.: Averaging using elliptic functions: approximation of limit cycles. *Acta Mech.* **81**, 125–142 (1990)
9. Vakakis, A.F., Rand, R.H.: Nonlinear dynamics of a system of coupled oscillators with essential stiffness non-linearities. *Int. J. Non-linear Mech.* **39**, 1079–1091 (2004)
10. Rand, R.H.: *Topics in Nonlinear Dynamics with Computer Algebra*. Gordon and Breach, Langhorne, PA (1994)
11. Guckenheimer, J., Holmes, P.: *Nonlinear Oscillations, Dynamical Systems, and Bifurcations of Vector Fields*. Springer, New York (1983)
12. Minorsky, N.: *Nonlinear Oscillations*. van Nostrand, Princeton, NJ (1962)